X-ray Diffraction

Kristen Zych*
University of Florida Department of Physics
(Dated: February 25, 2013)

In this experiment x-ray diffraction and absorption where studied. The device used emits x-rays of certain wavelengths, these are scattered off a crystalline sample, and finally collected by a Geiger-Mueller tube. The x-ray diffraction trials made use of three different crystalline samples that showed peaks of high photon counts when the Bragg condition was satisfied. Again using a crystal sample, x-ray absorption was investigated by placing a metal foil between the crystal and the detector. The metal foil allowed x-rays below a certain threshold through while blocking the absorbing the others, producing what is called an *absorption edge*.

1. INTRODUCTION AND THEORY

This lab was broken into two related parts: x-ray diffraction and x-ray absorption. The diffractometer created x-rays that could either be from $n = 2$ to $n = 1$ electron transitions or from $n = 3$ to $n = 1$ transitions; a more detailed explanation is in Section 2. These produce copper K_α x-rays that have a wavelength of $\lambda = 0.1542$ nm and K_β x-rays that have wavelengths of $\lambda = 0.1392$ nm, respectively [1]. There is also broad spectrum radiation that occurs from beam electrons slowing down as they hit the target; this is called *bremsstrahlung* radiation.

These x-rays pass through a slit and diffract off of a target crystal. If the x-rays impinge on the crystal at a certain angle, satisfying the *Bragg condition* (see Equation 1), then they constructively interfere and produce a peak in counts at the detector.

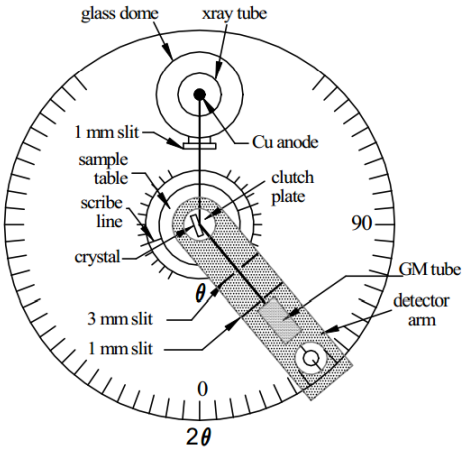

FIG. 1: Diffractometer schematic.

$$n\lambda = 2d\sin\theta \tag{1}$$

In the second part of the lab we placed metal foils in front of the detector to examine x-ray absorption.

2. APPARATUS AND EXPERIMENT

The apparatus we used is pictured in Figure 1. The diffractometer contained a copper anode that was used to create x-rays. A current through a tungsten filament creates an initial electron beam that excites the copper such that inner shell electrons would be kicked out by beam electrons. Then outer shell electrons fall into the newly vacant spots and in doing so, emits x-rays. As mentioned above, the these correspond to certain K_α and K_β x-rays. Figure 1 shows the basic path the collimated x-rays take: from the x-ray tube though a collimating slit to the crystal on the sample post, from there through two more slits to the GM tube. The arm of the diffractometer swings from about 15° to 120°, where this angle represents 2θ.

The software allowed us to set the step the arm of the apparatus either 1/2, 1/4, 1/8, or 1/16 degree steps. Also, the time spent on each step could be manipulated with regard to the intensity of the x-rays. High intensity warranted quick steps of 10 or 20 seconds while low intensity called for time steps of up to 100 seconds.

Three samples were put onto the pedestal, namely, LiF crystal, LiF powder, and KCl powder. The LiF crystal spectrum produced four peaks between 15° and 120° (see Appendix A: C.Q. 1, Figure 8 for details) since, using $a_0 = 0.403$ nm, Equation 1 is satisfied only four times in that range. The powder samples, however, satisfy this condition much more often due to "domains" of microcrystals. Consequently, the scattering is much weaker so the runs took about 30 hours. KCl is very similar to LiF in that they are both face-center-cubic, however, KCl is packed more closely. This fact produces interesting effects in the allowed Miller indices.

The absorption trials were taken with Zn, Cu, Ni, Co, Fe, Mn, Cr, and V foils. First a reference spectrum was taken and then each foil was placed in front of the GM detector in turn. From there, we were able to plot the ratio of the foil spectrum to the reference spectrum, which is also known as the transmittance.

*Electronic address: kzych@ufl.edu

Matched Peak	Scattering Angle		Appropriate Xray Wavelength	Miller Indices			Calculated Lattice Constant	
Estimate	2θ [°]	σ_2θ [°]	λ [nm]	h	k	l	a_m [nm]	σ_(a_m) [nm]
K_α1	39.06	0.03	0.1542	1	1	1	0.3995	0.0003
K_α2	45.39	0.08	0.1542	2	0	0	0.3997	0.0007
K_α3	66.09	0.09	0.1542	2	2	0	0.3999	0.0005
K_α4	79.39	0.07	0.1542	1	1	3	0.4004	0.0003
K_α5	83.55	0.10	0.1542	2	2	2	0.4009	0.0004
K_α6	100.59	0.21	0.1542	4	0	0	0.4009	0.0006
K_α7	113.46	0.21	0.1542	3	3	1	0.4020	0.0005
K_α8	118.26	0.14	0.1542	4	2	0	0.4017	0.0003
K_β1	35.23	0.14	0.1392	1	1	1	0.3984	0.0015
K_β2	40.64	0.21	0.1392	2	0	0	0.4008	0.0020
K_β3	59.04	0.17	0.1392	2	2	0	0.3995	0.0010
K_β4	70.26	0.17	0.1392	1	1	3	0.4012	0.0008
K_β5	74.13	0.13	0.1392	2	2	2	0.4000	0.0006

FIG. 2: This table displays the angular location of each peak in the LiF powder spectrum. It also shows the *hkl* values that correspond to each peak. Because LiF is face-center-cubic, *hkl* values can only either all even or all odd.

3. ANALYSIS AND RESULTS

3.1. Diffraction

We used the powder diffraction trials to determine the lattice constants of LiF and KCl. We did this by looking at the spectrum of peaks, taking note of the 2θ positions, and guessing based on height whether an individual peak was a K_α or K_β x-ray so that we know its wavelength. There also exists in the spectrum a low angle cut off wavelength λ_c that is representative of the fact that the machine only can produce 20 keV photons. Using Equation 2, we were able to determine an approximate value for a_0.

$$\lambda = \frac{2a_0}{\sqrt{h^2+k^2+l^2}} \sin\theta \tag{2}$$

The Miller indices h, k, and l classify which reflection is taking place, see Figure 2. While face-center-cubic lattice structures only allow either all even or all odd indices, some combinations of Miller indices produce a smaller intensity or no reflection because the x-rays are destructively interfering. A reflection's intensity is determined by the absolute square of the *crystal structure factor*, $F(hkl)$,

$$F(hkl) = \sum_j f_j e^{2\pi i(hu_j+kv_j+lw_j)} \tag{3}$$

where f_j is the type of atom at the site u_j, v_j, w_j.

We observed thirteen peaks for LiF powder (others were lost in the bremsstrahlung), assigned appropriate *hkl* values, and found that the value of a_m converged on the accepted value of $a_0 = 0.403$ nm at large angles.

Figure 3 shows the data and its fit. The fit was made using the following equation,

$$a_m = a_0 + c_1 g_1 + c_2 g_2 \tag{4}$$

where

$$g_1(\theta) = \frac{\cos^2\theta}{\sin\theta} \tag{5}$$

$$g_2(\theta) = \cos^2\theta \tag{6}$$

and a_0 is the accepted value of the lattice constant. The g_1 term dominates at small angles.

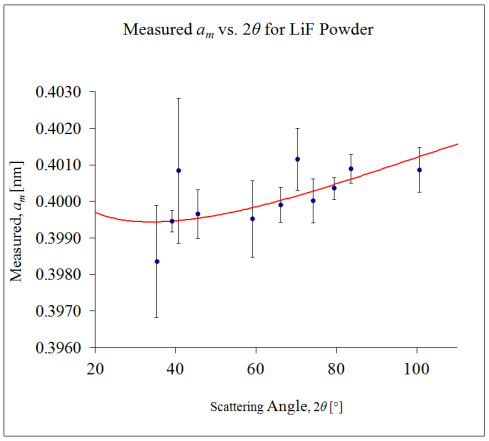

FIG. 3: Experimental data and fit of a_m for LiF as a function of the incident angle. The fit follows equation 4 with $c_1 = .0002$ and $c_2 = -.0046$.

For the KCl powder, Figure 4 tabulates the data. Because KCl powder is also effectively face-center-cubic, its Miller indices also had to either be all even or all odd. However, KCl is peculiar because it does not have $hkl =$ 111 or 311 reflections because of destructive interference (and presumably no higher order all-odd reflections)[2]. Similarly to the LiF data, the KCl data are converging on the accepted value of $a_0 = .629$ nm at large angles.[3]

Matched Peak	Scattering Angle		Appropriate Xray Wavelength	Miller Indices			Calculated Lattice Constant	
Estimate	2θ [°]	σ_2θ [°]	λ [nm]	h	k	l	a_m [nm]	σ_(a_m) [nm]
K_α1	29.11	0.12	0.1542	2	0	0	0.6136	0.0025
K_α2	41.33	0.09	0.1542	2	2	0	0.6179	0.0013
K_α3	51.16	0.08	0.1542	2	2	2	0.6186	0.0009
K_α4	59.88	0.13	0.1542	4	0	0	0.6179	0.0012
K_α5	67.50	0.12	0.1542	4	2	0	0.6206	0.0010
K_α6	74.81	0.09	0.1542	4	2	2	0.6218	0.0006
K_α7	95.58	0.25	0.1542	4	4	2	0.6246	0.0012
K_β1	26.42	0.11	0.1392	2	0	0	0.6091	0.0025
K_β2	37.37	0.05	0.1392	2	2	0	0.6145	0.0008

FIG. 4: This table displays the angular location of each peak in the KCl powder spectrum. It also shows the *hkl* values that correspond to each peak. Because KCl is face-center-cubic, *hkl* values can only either all even or all odd, however as mentioned above, some of the reflections are destroyed.

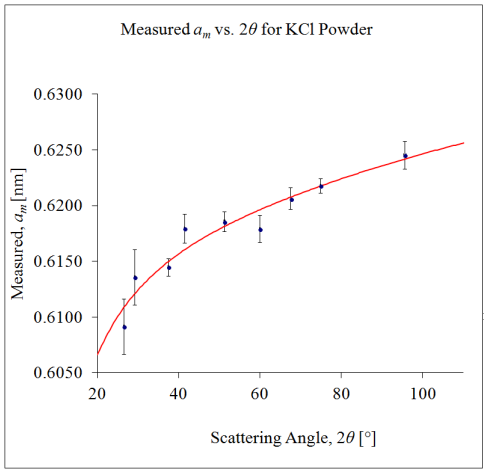

FIG. 5: Experimental data and fit of a_m for KCl as a function of the incident angle. The fit follows equation 4 with c_1=-.0028 and c_2=-.0068.

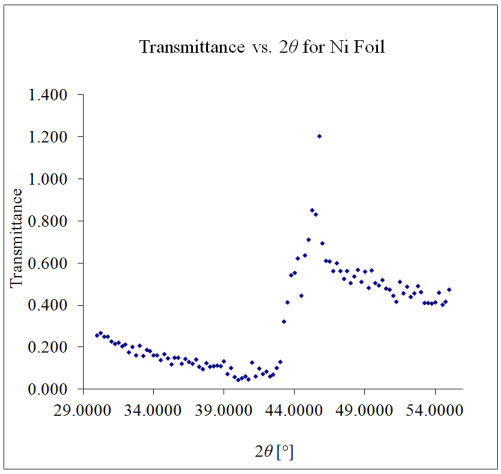

FIG. 6: The absorption edge of a Nickel foil.

3.2. Absorption

The absorption part of the lab is very similar to the diffraction part because we were still diffracting x-rays off a target crystal. However, now we placed six different metal foils in front of the detector and observed the change in the x-ray counts over a range of angles. As mentioned previously, we took reference spectra that were used for calculating the transmittance. These spectra spanned from, first, $30° < 2\theta < 55°$ with steps of $1/4°$ and 20 seconds per point, and secondly, $45° < 2\theta < 75°$ with steps of $1/8°$ and 100 seconds per point. The second spectrum (and it's subsequent metal foil comparisons) were longer runs than the manual suggested because we wanted to make sure we saw distinctly the absorption edge.

Shown in Figure 6 is the transmittance vs 2θ when a Nickel foil was between the crystal and the detector. Because $E \sim \frac{1}{\sin\theta}$, lower angles represent higher energies and vice versa. Nickel is particularly interesting because its absorption edge appears at approximately 44° which is in between were LiF crystal's first K_α (44.91°) and K_β (40.30°) pair. So in essence, you could use Nickel foil as a means to block K_β x-rays but not K_α's if the need presented itself. The other transmittance plots are located in Appendix A for your viewing pleasure.

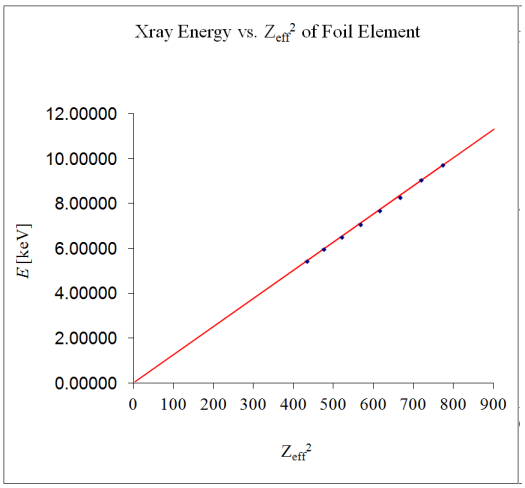

FIG. 7: X-ray energies at the point where absorption edges appear as a function of $(Z-1)^2$.

Contrary to intuition, every absorption edge plot shows

that the transmittance for a low energy x-ray is higher than the transmittance for a high energy x-rays. The energy of the x-ray where the edge appears is perfectly linear with the square of the effective Z, which is $Z-1$. This phenomena is shown in Figure 7.

4. CONCLUSIONS

For diffraction with LiF and KCl powders, the data shows how one can measure the lattice constant of a crystal using x-rays of known wavelength, scattering angles, and Miller indices. The Miller indices themselves help categorize what type of lattice the crystal is, whether is is simple cubic, body-center-cubic, face-center-cubic, or otherwise.

For x-ray absorption, the data showed that individual metals have their own absorption edges that is a function of their atomic number. It is possible that there is a multitude of different way error could have entered into the experiment. The most worrisome for us was that the tic marks on the diffractometer were not the same as what we were dialing into the software. However, on that note, every single one of our measurements deviated no more than 2% from accepted values.[3] Our Energy vs Z_{eff}^2 plot was very linear so we suspect that this source of error, and any other for that matter, were small enough to be ignored.

[1] R. Deserio, *X-ray Diffraction* (UF Physics Dept., 2012).
[2] B. D. Cullity, *Elements of X-ray Diffraction* (Addison-Wesley Pub. Co., Inc., 1956).
[3] Kaye and Laby, *4.2.1 X-ray absorption edges* (NPL, 2012).

APPENDIX A: COMPREHENSION QUESTIONS

1. C.Q. 1

The spectrum shows four peaks each at angles that satisfy the Bragg condition for copper K_α and K_β x-rays, where $d = a_0/2$. For the K_α peaks, we obtained a wavelength of 0.1539 nm for the first peak and 0.1549 nm for the second (Figure 8 on the next page summarizes the data).

2. C.Q. 2

A given hkl peak for 0.138 nm corresponds to at K_β x-ray. K_β x-rays occur when an electron makes a transition from n = 3 state to an n = 1 state. The reason you couldn't observe this peak without also observing a K_α peak of the same hkl is because, while K_β, is of higher energy, K_α x-rays are more frequent. Conversely, we saw many times the presence of K_α peaks but because the counts of K_βs were so low, they were lost in the Bremsstrahlung radiation.
For an NaCl structure, if the last $\lambda = 0.154$ (K_α) peak had hkl=331, then below it would be $hkl = 111$ and 311, because in this case only the all-odd reflections survive.

3. C.Q. 3

This is located in my lab notebook.

4. C.Q. 4

Figure 2 and 4 show our best estimates for the lattice constants for LiF and KCl and their uncertainties. The higher the intensity of the peak the more wrong the the calculation for a_0 was in both samples. This could be because systematic errors, such as the sample crystal being too far forward or backward or being turned slightly, since these errors are less apparent when 2θ becomes large. The values we came up with for c_1 and c_2 where very small. As was the value we got for the beam displacement D. We chose a representative value for c_1, measured a rough estimate for R, and made the calculation.

$$c_1 = -\frac{D}{R} \tag{A1}$$
$$D = Rc_1 \tag{A2}$$
$$D = (3.665\ cm)(-.003005) \tag{A3}$$
$$D = .011\ cm \tag{A4}$$
$$\tag{A5}$$

And .11 mm is not a terribly bad beam displacement.

5. C.Q. 5

The transmittance vs angle is related to the absorption vs wavelength in that below a certain angle transmittance in low, meaning above a certain energy absorption is high. This was briefly discussed in section 3.2. The reason absorption edges exist is because if the work function energy of photon gets to be too low (and the cut off is obviously sharp), it can no longer kick out electrons in the K shell and it is not absorbed. Instead they are transmitted. The transitions involved in the absorption is knocking a $n = 1$ state electron to infinity, or ionizing it. As mentioned previously, Ni absorbs K_β lines and Cobalt and Zinc absorb K_α lines. Copper, meanwhile lets

both lines through. Copper does not self-absorb its own K_α and K_β emissions because it needs enough energy to knock an electron to infinity. However, but definition, they energy available is limited to the energy gap between the $n = 1$ and $n = 2$ as well as the $n = 1$ and $n = 3$ gap.

Matched Peak	Scattering Angle		Measured Xray Wavelength	
Estimate	2θ [°]	σ_2θ [°]	λ_m [nm]	σ_(λ_m) [nm]
K_α1	44.91	0.05	0.1539	0.0002
K_α2	99.65	0.04	0.3079	0.0001
K_β1	40.30	0.05	0.1388	0.0002
K_β2	87.25	0.06	0.2780	0.0002
Cutoff	17.50	0.06	0.0613	0.0002

FIG. 8: K_α and K_β peaks for crystal LiF sample. Note: the wavelengths of the second peaks are listed as 2λ.

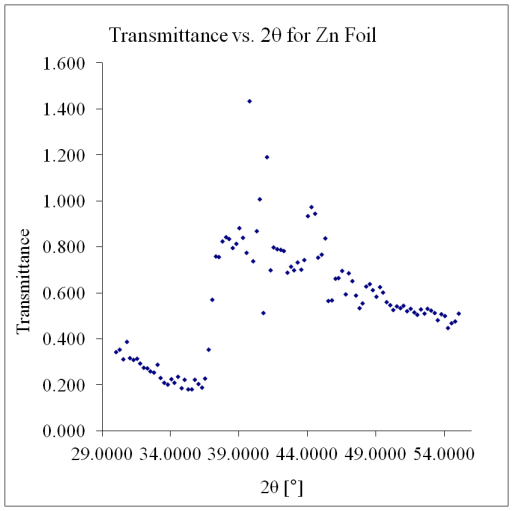

FIG. 9: Absorption edge for a Zn foil.

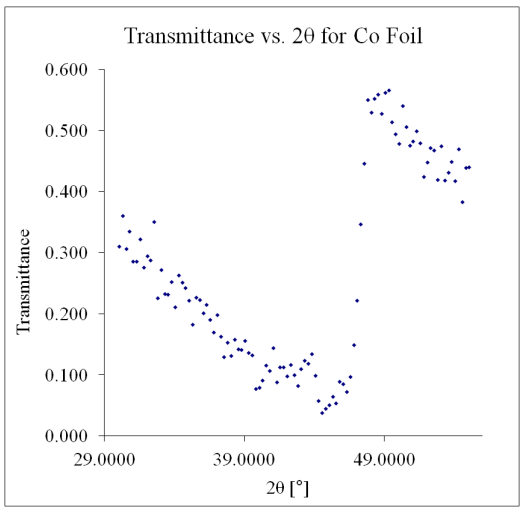

FIG. 10: Absorption edge for a Co foil.

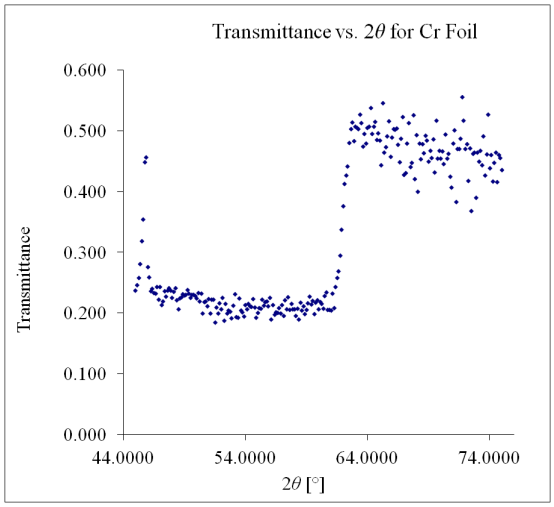

FIG. 11: Absorption edge for a Cr foil.

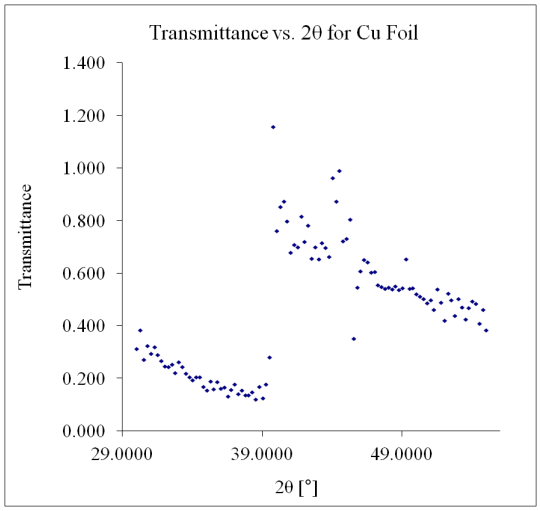

FIG. 12: Absorption edge for a Cu foil.

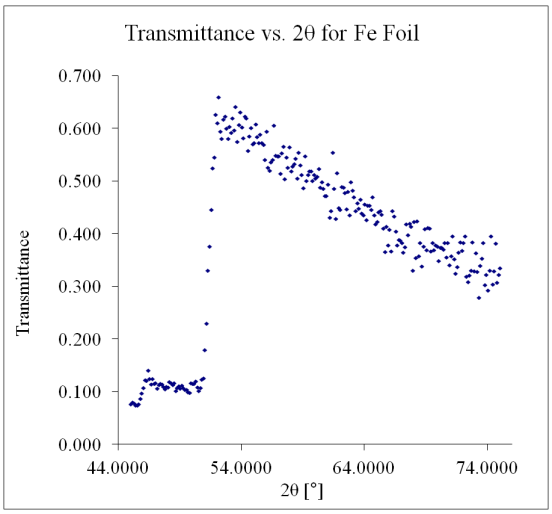

FIG. 13: Absorption edge for a Fe foil.

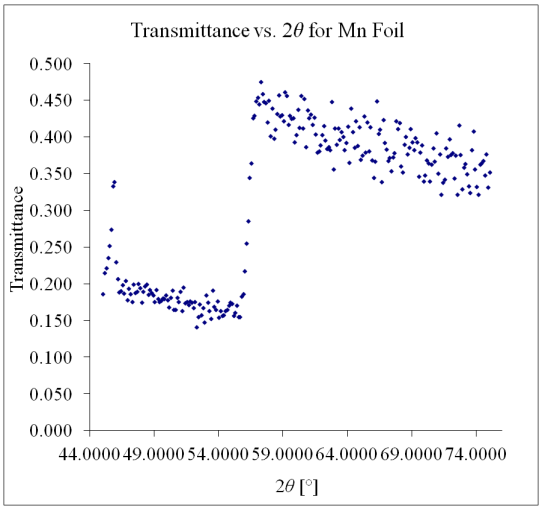

FIG. 14: Absorption edge for a Mn foil.

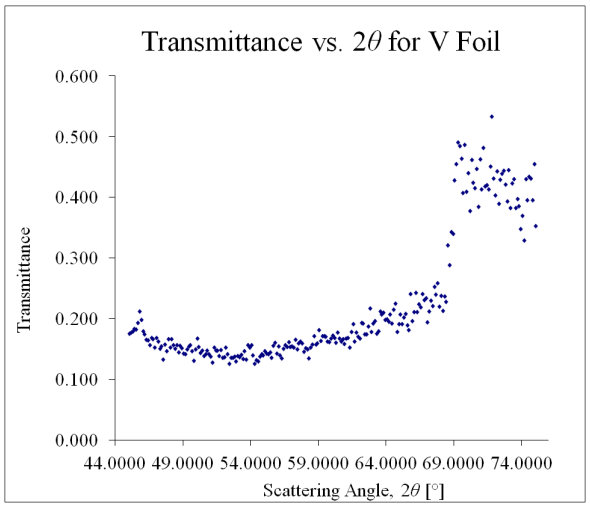

FIG. 15: Absorption edge for a V foil.